

## ความสัมพันธ์ของลักษณะทางเอกซเรย์คอมพิวเตอร์และการวัดเชิงปริมาณ กับการเกิดโรคการแตกของมะเร็งตับ

ณัฏฐา จิรอรำ ศิทธิพงศ์ ศรีสัจจาภูล  
ภาควิชารังสีวิทยา คณะแพทยศาสตร์ศิริราชพยาบาล มหาวิทยาลัยมหิดล

Received: November 14, 2021

Revised: December 27, 2021

Accepted: January 29, 2022

### บทคัดย่อ

โรคการแตกของมะเร็งตับ (Ruptured hepatocellular carcinoma) เป็นหนึ่งในภาวะแทรกซ้อนที่รุนแรงของโรคมะเร็งตับ วินิจฉัยโดยลักษณะจากการตรวจเอกซเรย์คอมพิวเตอร์ (Computed tomographic (CT) scan) เช่น การอยู่ชิดขอบของรอยโรค หรือรอยโรคยื่นออกนอกขอบเขตของตับ อย่างไรก็ตาม ยังมีการศึกษาเกี่ยวกับลักษณะทางเอกซเรย์คอมพิวเตอร์และการวัดเชิงปริมาณของโรคการแตกของมะเร็งตับที่ไม่มากนัก การศึกษาลักษณะในเอกซเรย์คอมพิวเตอร์และการวัดเชิงปริมาณของโรคการแตกของมะเร็งตับ เพื่อเป็นประโยชน์ในการวินิจฉัยที่ดีขึ้น การบอกรายกรณ์โรค และช่วงเวลาการรักษา การศึกษาข้อมูลหลังนี้ (retrospective study) ใช้กลุ่มตัวอย่างผู้ป่วยที่มีโรคการแตกของมะเร็งตับจำนวน 53 คน และกลุ่มควบคุมใช้ผู้ป่วยที่มีโรคมะเร็งตับที่ไม่มีการแตกของมะเร็งตับจำนวน 94 คน ศึกษาข้อมูลทางคลินิกและภาพเอกซเรย์คอมพิวเตอร์ของผู้ป่วยทั้งสองกลุ่ม ขนาดพื้นที่ ปริมาตรของรอยโรค ความยาวและความสูงการยื่นของรอยโรค มีค่าที่สูงกว่าในกลุ่มผู้ป่วยที่มีโรคการแตกของมะเร็งตับ ส่วนสัดส่วนการยื่น (protrusion ratio) และค่าความเข้มสีของเอกซเรย์คอมพิวเตอร์ (CT attenuation) มีค่าที่ต่ำกว่าอย่างมีนัยสำคัญในกลุ่มผู้ป่วยที่มีโรคการแตกของมะเร็งตับ การยื่นของรอยโรค การกระจายของโรคออกตับ การแพร่กระจายของโรค เส้นเลือดตับผิดปกติ น้ำในช่องห้อง การมีเนื้อตายของรอยโรค และการมีลิ่มเลือดอุดตันมีสัดส่วนที่มากกว่าในกลุ่มผู้ป่วยที่มีโรคการแตกของมะเร็งตับ โดยที่ความสูงการยื่นของรอยโรคมีความสัมพันธ์กับโรคการแตกของมะเร็งตับมากที่สุด ในการศึกษาหลายตัวแปรขนาดรอยโรคและการยื่นของรอยโรคมีความสัมพันธ์อย่างอิสระกับโรคการแตกของมะเร็งตับ และการยื่นของรอยโรคสัมพันธ์มากที่สุด โดยค่าจุดตัดขนาดของรอยโรค 6.3 เซนติเมตร ให้ค่าความไว้วยละ 88.7 และค่าความจำเพาะร้อยละ 73.4 ขนาดรอยโรคและการยื่นของรอยโรคมีความสัมพันธ์อย่างอิสระกับโรคการแตกของมะเร็งตับ โดยค่าจุดตัดขนาดรอยโรคที่มากกว่า 6.3 เซนติเมตร และความสูงการยื่นของรอยโรคมากกว่า 3 เซนติเมตรสัมพันธ์กับโรคการแตกของมะเร็งตับ

**คำสำคัญ:** การแตกของมะเร็งตับ ลักษณะเอกซเรย์คอมพิวเตอร์ การวัดเชิงปริมาณ

### ผู้นิพนธ์ประสานงาน:

ศิทธิพงศ์ ศรีสัจจาภูล  
ภาควิชารังสีวิทยา คณะแพทยศาสตร์ศิริราชพยาบาล มหาวิทยาลัยมหิดล  
2 ถนนวังหลัง แขวงศิริราช เขตบางกอกน้อย กรุงเทพมหานคร 10700  
อีเมล: tiam.mahidol@gmail.com

# Associated computed tomographic features and quantitative measurement of ruptured hepatocellular carcinoma

Nattawut Jiraaram, Sitthipong Srisajjakul

Department of Radiology, Faculty of Medicine Siriraj Hospital, Mahidol University

## Abstract

Ruptured hepatocellular carcinoma (HCC) is a life-threatening complication of liver cancer. The Computed Tomographic (CT) features of ruptured HCC confirmed the diagnosis of a peripherally located tumor with a contour bulge. The associated CT features and quantitative measurement are poorly understood. The assessment of the associated features of ruptured HCC may improve an accurate diagnosis, prognostic understanding, and treatment procedures. The associated CT features and quantitative measurement of ruptured HCC were retrospectively evaluated to improve accurate diagnosis and prognostic evaluation. The case group of 53 patients with ruptured HCC and the control group of 94 randomly selected HCC patients without ruptured tumors was clinically reviewed. The maximal tumor dimension, area, volume, protrusion length and height were greater in the rupture group, with the protrusion ratio and CT attenuation significantly lower. Tumor protrusion, extrahepatic invasion, metastasis, abnormal vascularity, ascites, necrosis and tumor thrombus were also significantly higher in the rupture group. Among the parameters, the protrusion height showed the highest association. Multivariable analysis determined that maximal tumor dimension and tumor protrusion were independently associated with ruptured HCC. Tumor protrusion showed the best correlation. Maximal tumor dimension at a cut-off value of 6.3 cm gave optimal sensitivity (88.7%) and specificity (73.4%). Maximal tumor dimension and tumor protrusion were independently associated with ruptured HCC. The maximal tumor dimension exceeded 6.3 cm and tumor protrusion height of more than 3 cm were suggestive of imminent HCC rupture.

**Keywords:** ruptured hepatocellular carcinoma, computed tomographic, quantitative measurement

## Corresponding Author:

**Sitthipong Srisajjakul**

Department of Radiology, Faculty of Medicine Siriraj Hospital, Mahidol University,  
2 Wanglang Road, Bangkok Noi, Bangkok 10700, Thailand.

E-mail: tiam.mahidol@gmail.com

## Introduction

Hepatocellular carcinoma (HCC) is an aggressive tumor and the most common type of chronic liver disease and cirrhosis.<sup>1</sup> HCC is the sixth most commonly diagnosed global cancer, with highest incidences (>10 per 100,000/year) observed in China, Southeast Asia including Thailand and sub-Saharan Africa. HCC is the second most common cause of cancer death in the world.<sup>2</sup> In Thailand, HCC is the most common cancer in men and the third most common in women.<sup>3</sup>

Ruptured HCC is a life-threatening complication that occurs in 3-15% of patients with HCC, with high mortality (25-75% in the acute phase) and liver failure (12-42% in the acute phase).<sup>4,5</sup>

Diagnosis of ruptured HCC is performed by laboratory investigation (abdominal paracentesis) or imaging (such as a computed tomographic (CT) scan (most sensitive imaging)). A CT scan suggests rupture of HCC by a peripherally located tumor with a contour bulge, discontinuity of the liver capsule, hemoperitoneum, subcapsular hematoma, active extravasation of contrast and enucleation sign.<sup>6,7</sup> However, the mechanism of HCC rupture and quantitative characteristics of the tumor are poorly understood.

## Objectives

Assessing the associated features of ruptured HCC could improve diagnosis, prognostic evaluation, and treatment procedures. This retrospective study examined associated CT features and quantitative

measurement of ruptured HCC during a 3-year period at a single center in Thailand. Results may lead to better evaluation of ruptured HCC diagnosis and prognostic evaluation in asymptomatic patients.

## Materials and methods

This retrospective case-control study was performed during a 3-year period at a single center in Thailand. The research methodology was approved by the Ethics Committee of the Faculty of Medicine, Siriraj Hospital, Bangkok, Thailand.

## Patient selection

All patients with a history of HCC were retrospectively reviewed using data from the Institutional Radiology Department reporting system and Picture Archiving and Communication System (PACS) between January 2017 and May 2020.

HCC was diagnosed by typical radiologic imaging examinations showing the characteristic features.<sup>8,9</sup> Ruptured HCC was diagnosed by identifying HCC with hemoperitoneum, surrounding perihepatic hematoma, active extravasation of contrast materials, tumor protrusion from the hepatic surface, focal discontinuity of the hepatic surface or an enucleating sign.<sup>7,10</sup>

Patients with uncertain diagnosis and those with missing clinical data or incomplete phase of CT study (noncontrast, late arterial and portovenous phases) were excluded.

Selected patients were divided into two groups as with and without ruptured HCC.

The case group comprised 53 patients with clinical/radiographic evidence of ruptured HCC, while the control group consisted of 94 HCC patients without previous treatment of interesting lesions (such as TACE, RFA or chemotherapy) or clinical/radiographic evidence of ruptured HCC with at least a 4-month follow-up. Patients were randomly selected from eligible lists.

Clinical information, demographics and radiologic findings of all 147 patients were successfully reviewed.

#### **Preprocedure CT**

Diagnostic CT scans were conducted in the hospital (120 kVp; 300 mA; section thickness, 1.25 mm; pitch, 1.735:1) on a 64-slice CT scanner (GE Light speed VCT), (GE Discovery) and a 256-MDCT (GE revolution CT). Patients received IV contrast medium 2 ml/kg. of body weight with injection rate of 3 ml/second.

#### **Data collection**

Demographic data (age and sex), previous treatment and duration of treatment were recorded.

Radiologic findings were reviewed by an in-training diagnostic radiology resident for features, characteristics and quantitative measurements as (a) site of tumor (right, left or both lobes), (b) (largest or ruptured) tumor dimension in three planes (anteroposterior (AP), width (W), height (H)), (c) presence of protrusion of the tumor, length and height of protruded margins of the tumor, maximal protrusion plane, (d) presence of extrahepatic

invasion (associated thickening of the contiguous diaphragm or abdominal wall), (e) presence of ascites, (f) cirrhosis, (g) extrahepatic metastasis, (h) intratumoral abnormal vascularity (such as pseudoaneurysm), (i) intratumoral necrosis area, (j) tumor thrombus in the hepatic vein (HV) or other vessels and (k) tumor CT attenuation in the arterial and portovenous phases. Equivocal or uncertain findings were reviewed and discussed to obtain a consensus among senior abdominal radiology staff.

Tumor area and volume were calculated by the formulas:  $\pi/4 \times AP \times W$  and  $4/3 \pi \times AP \times W \times H$ .<sup>11,12</sup> Tumor CT attenuation in arterial to portovenous phase ratio and protrusion length to height ratio were also calculated.

Tumor protrusion was determined from a CT image slide of maximal tumor dimension on each plane (axial, coronal and sagittal). Length and height of protruded tumor margins were measured along the protruded segment (Figure 1A). When the tumor protruded along more than one surface, the length and height of protrusion were obtained by adding the value of each protrusion (Figure 1B). Maximal value among the three planes was selected to represent length and height of tumor protrusion.

An example of the tumor measurements was demonstrated in Figure 2.

#### **Statistical analysis**

Data were prepared and analyzed using PASW Statistics 18.0 (SPSS Inc., Chicago IL USA). Continuous data were reported as

mean and standard deviation or median as minimal and maximal where appropriate and compared using the Student t test or the Mann-Whitney U test. Discontinuous data were reported as percentage and compared using the Chi-squared test. Multivariate analyses were performed using binary logistic regression. Differences were considered significant at a p-value of 0.05. Receiver operating characteristic

(ROC) analysis was used to determine the area under the curve (AUC) to assess the diagnostic accuracy of maximal tumor dimension, tumor area, tumor volume, tumor protrusion length, height and ratio in the prediction of ruptured HCC. Diagnostic accuracy of optimal cutoff values for ROC analysis was ensured by maximizing sensitivity and specificity.

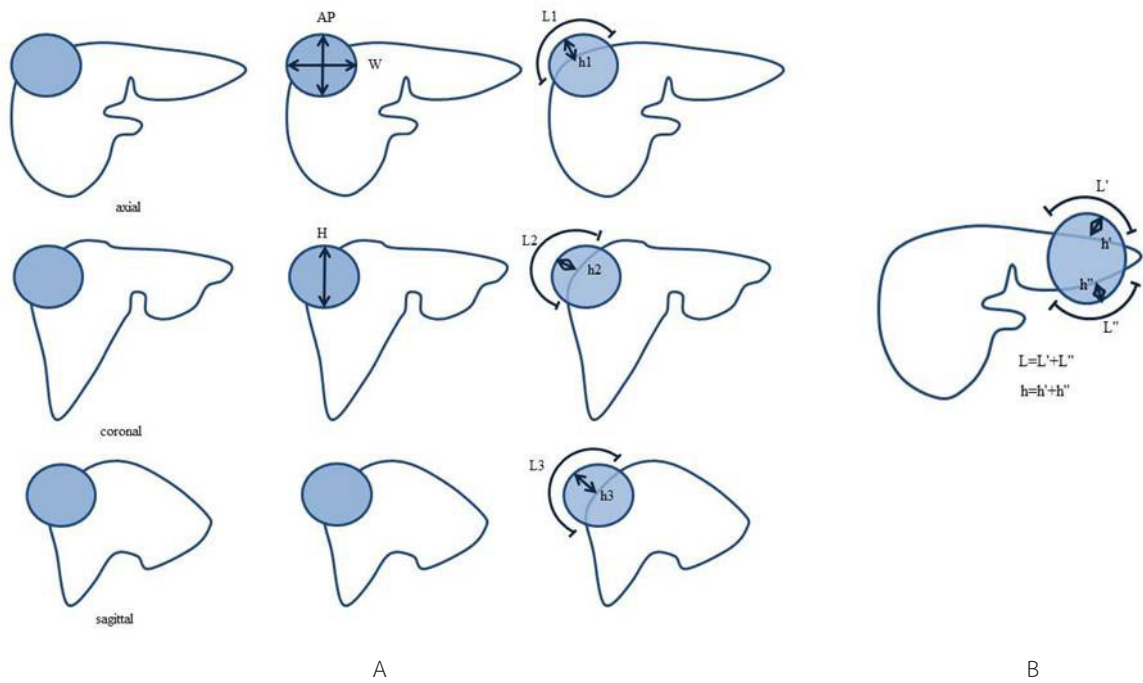


**Figure 1:**

A - Dimension and protrusion measurement method based on slide of maximal tumor dimension in each plane. Maximal values from L1, L2, L3 and h1, h2, h3 were selected as representative. B - Protrusion measurement method. If the tumor protruded along more than one surface, the length and height of protrusion were obtained by adding the value of each protrusion (adapted from Kanematsu et al.).<sup>11</sup>

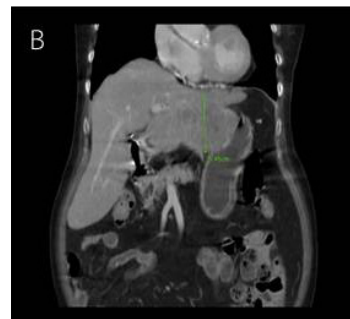
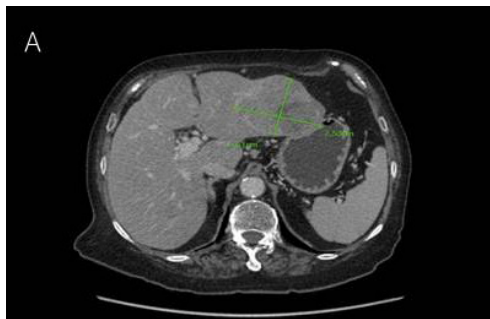


**Figure 2:** An 81-year-old woman with a history of abnormal AFP level and first diagnosed HCC without clinical or radiographic evidence of ruptured tumor

A, B - CT images showing a heterogeneously enhanced mass with internal necrotic portion at left lobe, measuring 7.5x5.1x5.4 cm.

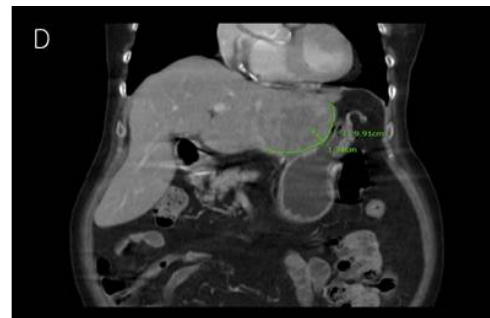
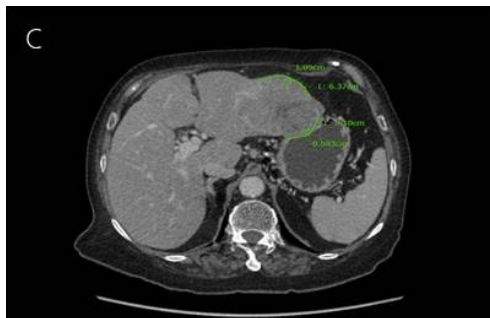


**Figure 3: C, D - Protrusion quantitative measurement** was performed on axial and sagittal planes at image slide of maximal tumor diameter (no demonstrated tumor protrusion on the sagittal plane). On the axial plane (image C), the tumor protruded along more than one surface. Length (L) and height (H) of protrusion were obtained by adding the value of each protrusion ( $L = 6.37 + 5.10 = 11.47$  cm,  $H = 1.05 + 0.59 = 1.64$  cm). On the coronal plane (image D), the length and height of protrusion were 9.91 cm and 1.31 cm, respectively. Maximal protrusion measurements among all planes as 11.47 cm and 1.64 cm for length and height of protrusion, respectively were selected as representative.

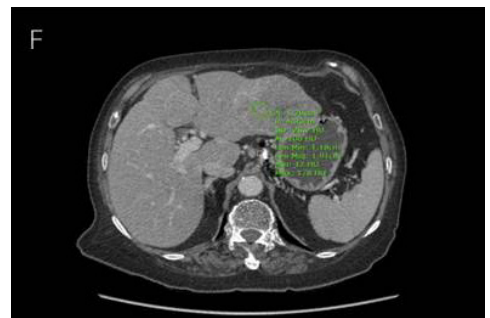


**Figure 4:** E, F - CT attenuation measurement in both arterial and portovenous phases

## Results

The rupture group and non-rupture group consisted of 40 men, 13 women and 71 men, 23 women, respectively. Mean ages of the rupture group and non-rupture group were  $60.51 \pm 12.904$  and  $63.22 \pm 10.610$  years. Previous treatment was found in the rupture group at 22.6% and in the non-rupture group at 5.3%. Frequency of tumor location in both rupture and non-rupture groups was right lobe,

then left lobe and both lobes. Maximal tumor protrusion plane in the rupture group was coronal (43.5%) followed by sagittal (43.5%), with axial (13.0%). In the non-rupture group, maximal tumor protrusion plane was coronal (53.3%) followed by sagittal (30.0%) and axial (16.7%). Most patients in the non-rupture group (91.5%) were treated with various modalities including RFA, TACE and surgical resection with median treatment duration 43.5 days.

**Table 1** Demographic Data of All Patients

	Total (n=147)	Ruptured vs non-ruptured HCC		p-value
		Rupture (n=53)	Non-rupture (n=94)	
Sex				0.993
Male	111 (75.5%)	40 (75.5%)	71 (75.5%)	
Female	36 (24.5%)	13 (24.5%)	23 (24.5%)	
Age (year)	$62.24 \pm 11.520$	$60.51 \pm 12.904$	$63.22 \pm 10.610$	0.171
Previous treatment	17 (11.6%)	12 (22.6%)	5 (5.3%)	0.002
Location				0.001
Right lobe	105 (71.4%)	31 (58.5%)	74 (78.7%)	
Left lobe	33 (22.4%)	14 (26.4%)	19 (20.2%)	
Both lobe	9 (6.1%)	8 (15.1%)	1 (1.1%)	
Maximal protrusion plane				0.496
Axial	11 (14.5%)	6 (13.0%)	5 (16.7%)	
Coronal	36 (47.4%)	20 (43.5%)	16 (53.3%)	
Sagittal	29 (38.2%)	20 (43.5%)	9 (30.0%)	
Duration to treatment (day)	-	-	43.50 (2,668)	

Values presented as frequency (%), mean  $\pm$  SD and median (minimum, maximum). *p*-value corresponds to Independent's t test (Continuous data) and Chi square test (Categorical data)

CT measurements in both rupture and non-rupture groups are compared in Table 2. Maximal tumor dimension, tumor area, tumor volume, protrusion length and height ratio were significantly greater ( $p<0.05$ ) in the rupture group. Protrusion length, height and length: height ratio and protrusion height were the most associated at  $p<0.001$ . CT attenuation

in both arterial and portovenous phases of the rupture group were significantly lower than for the non-rupture group.

Protrusion frequency of the tumor, extrahepatic invasion, metastasis, abnormal vascularity, ascites, necrosis and tumor thrombus in the hepatic vein and other vessels were also significantly higher in the rupture

group than in the non-rupture group. Cirrhosis was not significantly correlated with occurrence of rupture (Table 2).

Multivariable analysis, using binary logistic regression, indicated association of the CT features with rupture. The two independent variables as maximal tumor dimension and tumor protrusion correlated best with ruptured HCC ( $p<0.001$ ).

The ROC analysis for maximal tumor dimension, tumor area, tumor volume, protrusion length, height and ratio yielded AUCs of 0.870 (95% CI: 0.815-0.926;  $p<0.001$ ), 0.863 (95% CI: 0.806-0.919;  $p<0.001$ ), 0.867 (95% CI: 0.811-0.923;  $p<0.001$ ), 0.722 (95% CI: 0.602-0.843;  $p<0.001$ ), 0.751 (95% CI: 0.631-0.871;  $p<0.001$ ) and 0.691 (95% CI: 0.566-0.817;  $p=0.005$ ), respectively (Table 3).

Cutoff values for each quantitative measurement were selected from the ROC

analysis that yielded maximal sensitivity and specificity. Different diagnostic accuracies of each measurement with selected cutoff values are shown in Table 3. Tumor volume at cutoff value 800 cm<sup>3</sup> gave optimal sensitivity and specificity to predict ruptured HCC. Among the significant two independent variables, maximal tumor dimension at cutoff value 6.3 cm gave optimal sensitivity and specificity to predict ruptured HCC (AUC 0.870, 95% CI 0.815-0.926, sensitivity 88.7%, specificity 73.4%). Protrusion height at cutoff value 3 cm also showed good sensitivity and specificity with AUC 0.751, 95% CI 0.631-0.871, sensitivity 78.3%, specificity 63.3% but inferior to maximal tumor dimension.

However, the distribution of values between rupture and non-rupture groups still showed overlaps (Figure 3).

**Table 2** Associated CT features of Ruptured HCC

	Univariate analysis*			Multivariate analysis**	
	Rupture	Non-rupture	p-value	OR (95% CI)	p-value
Maximal dimension (cm)	11.78 (3.69, 33.56)	3.37 (1.00, 20.12)	<0.001	1.227 (1.048-1.435)	0.011
Area (cm <sup>2</sup> )	70.69 (8, 286)	5.92 (1, 170)	<0.001		
Volume (cm <sup>3</sup> )	3,859.04 (126, 51,119)	95.29 (3, 18225)	<0.001	1.804 (0.373-8.732)	0.463
Protrusion	46 (86.8%)	29 (30.9%)	<0.001	7.630 (2.235-26.049)	0.001
Length (cm)	17.22 (5.39, 79.00)	9.46 (1.43, 32.26)	0.001		
Height (cm)	5.12 (1.23, 24.20)	2.12 (0.36, 12.00)	<0.001		
Length: height ratio	3.49 (2.13, 8.25)	4.54 (2.39, 12.22)	0.005		
CT attenuation					
Arterial (HU)	86.23±29.46	99.38±30.61	0.013	0.992 (0.97-1.013)	0.474
Portovenous (HU)	82.07±21.12	93.97±22.02	0.002	0.981 (0.953-1.011)	0.208
Arterial: portovenous ratio	1.08±0.47	1.03±0.30	0.395		

**Table 2 (Con.)**

	Univariate analysis*			Multivariate analysis**	
	Rupture	Non-rupture	p-value	OR (95% CI)	p-value
Cirrhosis	39 (73.6%)	62 (66%)	0.338		
Extrahepatic extension	4 (7.5%)	1 (1.1%)	0.037		
Metastasis	14 (26.4%)	1 (1.1%)	<0.001		
Abnormal vascularity	28 (52.8%)	12 (12.8%)	<0.001	1.565 (0.495-4.949)	0.446
Ascites	50 (94.3%)	10 (10.6%)	<0.001		
Necrosis	53 (100%)	56 (59.6%)	<0.001		
Thrombus in hepatic vein	18 (34%)	9 (9.6%)	<0.001	0.397 (0.093-1.702)	0.214
Thrombus in other vessels	30 (56.6%)	13 (13.8%)	<0.001	1.582 (0.462-5.420)	0.466

\*Values presented as frequency (%), mean  $\pm$  SD and median (minimum, maximum). P-value corresponds to Independent's t test (Continuous data) and Chi square test (Categorical data)

\*\*Values presented as Odds ratio (OR) and 95% Confident Interval (CI). P-value corresponds to Logistic regression analysis

**Table 3** ROC curve analysis, cutoff level and diagnostic accuracy of associated CT features of ruptured HCC

Parameter	AUC (95% CI)	Sensitivity	Specificity
Max dimension (cm) cutoff value = 6.3	0.870 (0.815-0.926)	88.7%	73.4%
Area (cm <sup>2</sup> ) cutoff value = 24	0.863 (0.806-0.919)	86.8%	74.5%
Volume (cm <sup>3</sup> ) cutoff value = 800	0.867 (0.811-0.923)	86.8%	75.5%
Protrusion length cutoff value = 10	0.722 (0.602-0.843)	84.8%	53.3%
Protrusion height cutoff value = 3	0.751 (0.631-0.871)	78.3%	63.3%
Protrusion LH ratio cutoff value = 3.8	0.691 (0.566-0.817)	32.6%	36.7%

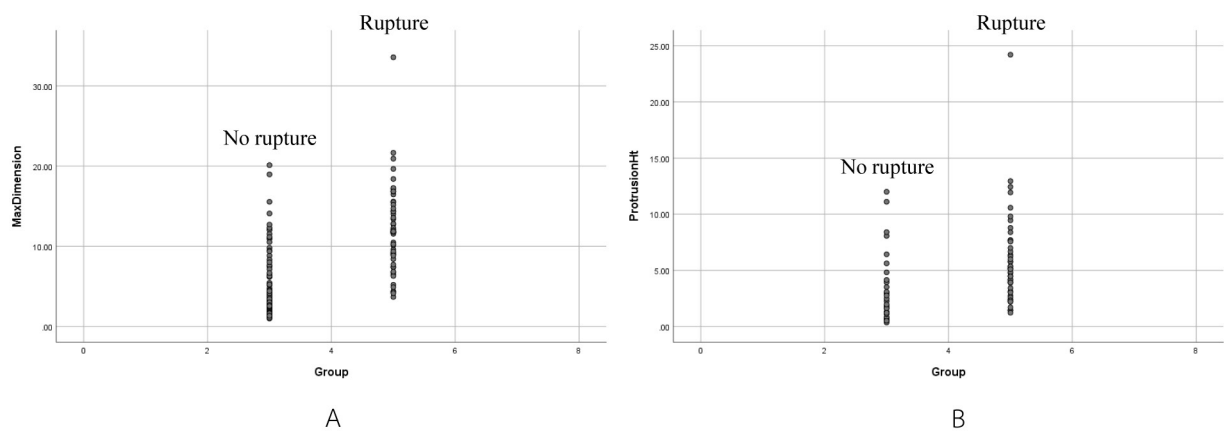


**Figure 5:** Distribution of CT measurements for groups with and without rupture of hepatocellular carcinoma.

A: Maximal tumor diameter on CT scans

B: Maximal protrusion height of tumor on CT scans

## Discussion

Rapid tumor growth was hypothesized as an indication of immanent HCC rupture.<sup>4,13</sup> In a previous study, tumor size was found to be a significant risk factor of ruptured HCC,<sup>14</sup> and tumor size greater than 5-7 cm predicted imminent HCC rupture.<sup>11,13</sup> Our results also showed significantly higher tumor dimension in the ruptured HCC group and maximal tumor dimension, with a cutoff value of 6.3 cm, giving optimal sensitivity and specificity for ruptured HCC prediction.

Univariable analysis showed that tumor area and tumor volume were also significantly higher in the rupture group. However, no significant differences between these factors were determined by multivariable analysis because tumor area and volume were dependent factors of tumor dimension.

The protruding contour of the tumor is a well-known method for diagnosis of HCC rupture.<sup>10</sup> Some studies observed that the protruding contour value was significantly associated with HCC rupture.<sup>11,13,15</sup> Similar to our results, significantly higher protrusion measurement parameters were seen in the rupture group. Protrusion height showed the greatest association with HCC rupture among all protrusion parameters. For slightly protruded tumor contours, high protrusion length occurred due to the large area of the slightly protruded tumor. Therefore, protrusion length had less association with ruptured HCC and was not a good indicator for tumor contour bulging.

Few studies have investigated protrusion quantitative measurement. Our study showed that protrusion height at cutoff

value of 3 cm gave good sensitivity and specificity for ruptured HCC prediction but was inferior to maximal tumor dimension.

All tumors in the rupture group presented a necrotic area with significant association. This finding was consistent with spontaneous rupture hypotheses of rapid tumor growth and necrosis.<sup>4,6,13</sup> Lower CT attenuation was found in both arterial and portovenous phases in the rupture group, possibly resulting from a hypodense necrotic area in large or rapid growth tumors, while the non-significant difference in multivariable analysis of CT attenuation was due to tumor dimension dependency.

Extrahepatic extension, metastasis and ascites were also significantly associated with the rupture group. These results were inconsistent with Kanematsu et al.<sup>11</sup>, possibly due to the early stage of HCC detection in current clinical practice, resulting in lower frequency of ascites, extrahepatic extension and metastasis in our control group.

Tumor thrombus venous vessels and abnormal vascularity (intratumoral pseudoaneurysm) were significantly associated with the rupture group. These findings were explained by increased intratumor pressure, with occlusion of hepatic veins by tumor thrombi or invasion causing spontaneous ruptured HCC<sup>4,6,13</sup> and tumoral neoangiogenesis as a marker of aggressive tumor growth.<sup>16</sup> However, these factors showed no significant association in multivariable analysis due to tumor size dependency.<sup>16</sup>

There were some research limitations. This retrospective study was conducted at a single center in Thailand. Numbers of the case group that underwent a recent CT study before the rupture event were limited for direct evaluation of the CT predictor of a subsequent rupture event. Significant differences, with good sensitivity and specificity, were shown in maximal tumor diameter and protrusion height but distribution of values between the rupture and non-rupture groups gave significant overlaps.

## Conclusions

Maximal tumor dimension and tumor protrusion were independently associated with HCC rupture. Maximal tumor dimension at a cutoff value of 6.3 cm gave optimal sensitivity and specificity with AUC 0.870, 95% CI 0.815-0.926, sensitivity 88.7%, specificity 73.4%. Among all protrusion parameters, protrusion height gave optimal association with ruptured HCC. Maximal tumor dimension at more than 6.3 cm and tumor protrusion height of more than 3 cm were suggestive CT findings of ruptured HCC. When high associated ruptured HCC CT findings are observed in asymptomatic patients, early preventative therapeutic intervention may be considered.

## Acknowledgment

We would like to express our sincere gratitude to Julaporn Pooliam, MSc. for guidance and assistance with research methodology and statistical analysis.

## References

1. Abdalla EK, Stuart KE. Overview of treatment approaches for hepatocellular carcinoma [Internet]. Up To Date. [cited 2020 Oct 18]. Available from: <https://www.uptodate.com/contents/overview-of-treatment-approaches-for-hepatocellular-carcinoma>.
2. Torre LA, Bray F, Siegel RL, et al. Global cancer statistics, 2012: Global Cancer Statistics, 2012. *CA Cancer J Clin* 2015;65:87-108.
3. Somboon K, Siramolpiwat S, Vilaichone R-K. Epidemiology and survival of hepatocellular carcinoma in the central region of Thailand. *Asian Pac J Cancer Prev* 2014;15:3567-70.
4. Lai ECH, Lau WY. Spontaneous rupture of hepatocellular carcinoma: a systematic review: A systematic review. *Arch Surg* 2006;141:191-8.
5. Zhu Q, Li J, Yan JJ, et al. Predictors and clinical outcomes for spontaneous rupture of hepatocellular carcinoma. *World J Gastroenterol* 2012;18:7302.
6. Sahu SK, Chawla YK, Dhiman RK, et al. Rupture of Hepatocellular Carcinoma: A review of literature. *J Clin Exp Hepatol* 2019;9:245-56.
7. Singhal M, Sinha U, Kalra N, et al. Enucleation sign: A computed tomographic appearance of ruptured hepatocellular carcinoma. *J Clin Exp Hepatol* 2016;6:335-6.
8. Choi J-Y, Lee J-M, Sirlin CB. CT and mr imaging diagnosis and staging of hepatocellular carcinoma: Part I. development, growth, and spread: Key Pathologic and imaging aspects. *Radiology* 2014;272:635-54.
9. Santillan C. CT and MRI of the liver for hepatocellular carcinoma. *Hepatoma Res* 2020;6:63.
10. Kim HC, Yang DM, Jin W, et al. The various manifestations of ruptured hepatocellular carcinoma: CT imaging findings. *Abdom Imaging* 2008;33:633-42.
11. Kanematsu M, Imaeda T, Yamawaki Y, et al. Rupture of hepatocellular carcinoma: predictive value of CT findings. *AJR Am J Roentgenol* 1992;158:1247-50.
12. Kashkoush S, El Moghazy W, Kawahara T, et al. Three-dimensional tumor volume and serum alpha-fetoprotein are predictors of hepatocellular carcinoma recurrence after liver transplantation: refined selection criteria. *Clin Transplant* 2014;28:728-36.
13. Xia F, Ndhlovu E, Zhang M, et al. Ruptured hepatocellular carcinoma: Current status of research. *Front Oncol* 2022;12.
14. Kerdsuknirun J, Vilaichone V, Vilaichone R-K. Risk factors and prognosis of spontaneously ruptured hepatocellular carcinoma in Thailand. *Asian Pac J Cancer Prev* 2018;19:3629-34.
15. Choi BG, Park SH, Byun JY, et al. The findings of ruptured hepatocellular carcinoma on helical CT. *Br J Radiol* 2001;74:142-6.

16. Trevisani F, Cantarini MC, Wands JR, et al.  
Recent advances in the natural history of  
hepatocellular carcinoma. *Carcinogenesis*  
2008;29:1299-305.